



## ENHANCE NON-IDEAL IRIS RECOGNITION SYSTEM FROM NIR IRIS VIDEO

<sup>1</sup>NUR KHDER NSEAF, <sup>2</sup>AZRULHIZAM SHAPII, <sup>3</sup>ASAMA KUDER NSEAF, <sup>4</sup>AZIZAH JAAFAR,  
<sup>5</sup>KHIDER NASSIF JASSIM, <sup>6</sup>AHMED KHUDHUR NSAIF

<sup>(1&2)</sup>School of Information Technology, Faculty of Information Science and Technology,  
Universiti Kebangsaan Malaysia, Malaysia

<sup>(3&4)</sup>Institute of Visual Informatics (IVI), Universiti Kebangsaan Malaysia, Malaysia

<sup>5</sup>Faculty of Management and Economics Department of Statistics University of Wasit Al-Kut, Iraq

<sup>6</sup>Department of Electrical, Electronic & Systems Engineering, Faculty of Engineering & Built  
Environment, Universiti Kebangsaan Malaysia, Malaysia

<sup>1</sup>noorkhuder201@gmail.com, <sup>2</sup>azrulhizam@ukm.edu.my, <sup>3</sup>osama\_ftsm@yahoo.com,  
<sup>4</sup>azizahj@ukm.edu.my, <sup>5</sup>khder.albayati@gmail.com, <sup>6</sup>ahmed.eng.communication@gmail.com

### ABSTRACT

Iris pattern is one of the most consistent biometric methods used for recognizing and identifying persons. Employing videos as a capturing instrument is a pretty modern style in the area of iris biometric. The use of frame by frame method provides more information and offers more suppleness compared to old-fashioned still images. Nevertheless, the size, quality and shape of the iris might differ between a frame and another. Additionally, to getting best performance it need a rapid and precise method to segment iris to amelioration rate of recognition. This work presents a method for choosing the best frames found in an iris video. This method is based on detecting motion blur and occlusion in iris videos and investigating their influence on the process of recognition. This proposed is followed by a rapid and precise method to detect pupil area, this method on the grounds of “dynamic threshold” with “Circular Hough Transform” then apply “Geodesic Active Contour” for detect outer boundary of iris. Experimental results are carried out on the MBGC NIR Iris Video datasets from the National Institute for Standards and Technology (NIST). Results show that the suggested selection method in NIR Iris Videos results in substantial enhancement in recognition efficiency. Results also indicated that the experimental evaluation of Iris segmented technique proposed in this work indicates that the precision and speed of the iris recognition via video is improved.

**Keywords:** *Iris Biometrics, Video Iris Recognition, Pupil Segmentation, Non-Ideal Iris Recognition, GAC Iris Segmentation*

### 1. INTRODUCTION

Iris recognition is one of the fields that witnesses rapid development as a fertile research area [2]. Consequently, numerous scholars have become more involved in developing iris recognition to be suppler, quicker, and more consistent. In spite of the huge quantity of fresh research in the field of iris biometrics, previous works have focused largely on still iris images.

Daugman [4–7], Wildes [30], Boles and Boashash [1], Ma et al. [16, 17] and others [19; 21; 24-25; 27–29] offered various iris recognition structures. These structures are planned to operate on iris images obtained via an inflexible imagery set-up.

Iris biometric develops to move from the use of still-images to video-images that addresses some of the limitations previously confronted when using still images. On the other hand, the utilization of video-images has brought along different some serious issues that require extra consideration. It has been well stated that a still image cannot be constantly optimal with regard to quality, as it rather contains several forms of noise such as specular highlights, reflections and occlusions [2] [13] [18]. These insufficiencies in previous methods of image capturing and recognition entail the presentation of several improvement procedures. One of these enhancing procedures is the iris videos which is a more flexible technique that offers several frames to select from instead of the limited



ones offered in still images techniques [34]. Nonetheless, some frames taken via videos are possibly out the focus and perhaps occluded. Other frames might be sharp and of good quality. Furthermore, the processing of frames requires more effective methods because of extra numbers of frames.

Zhou and Chellappa [31] stated that utilizing video may enhance the performance of face recognition techniques. The present study assumes that utilizing such practices for iris recognition might produce better performance as well. Several prior researches in iris recognition area such as [8] [9] [14] [17] [26] have used multiple still images.

The use of single still images has suffered several limitations. One limitation of this kind of still images is that it often results in a modest quantity of noise. Specular highlights and eyelash occlusion can lessen the quantity of iris texture data found in this kind of image. Conversely, an iris video clip results in a specular highlight in one of the frames but not necessarily appear in the next frame. Furthermore, eyelash occlusion amount is not fixed all over the frames. A better image can be captured via various frames extracted from a video to produce one pure iris image. Another limitation detected in still images is that variations in lighting may lead to higher Hamming distance score compared to the one found in between two stills. Variations resulting from variations in lighting can be reduced through merging information from various frames of a video.

Zhou and Chellappa [31] proposed considering averages to incorporate texture information through multiple video frames to enhance face recognition efficiency. The combination of multiple images will smooth away the noise detected and the relevant texture will be preserved. In this paper, a method is presented to select best frames from an iris video. The proposed experiments illustrated that that our method can improve iris recognition efficiency. We present an optimization method for pupil segmentation that our experiments show that faster and accurate pupil segment. In additionally, to perform iris segment we apply the Geodesic Active Contour (GAC) algorithm by Shah and Ross [28] and an open source masek [19] method to comparing between them.

This work is ordered as follows; section 2 reviews related works, section 3 describes the data created in this study, section 4 explains what is meant by iris segmentation. Normalization, encoding and matching procedures are designated in Sections 5, 6, 7 respectively. Results of experiments conducted and their discussion

together with the comparison between the suggested method and some previous methods are all provided in section 8. Section 9 summarizes the basic conclusions of this study.

## 2. RELATED WORKS

Zhou and Chellappa [31] surveyed several techniques which used video in face biometrics. Video has been successfully employed to enhance face recognition performance. Nevertheless, very little research has been exerted on the use of video in iris biometrics. Aiming at encouraging the exploration of iris biometrics using unrestricted video, government of the U.S planned for the Multiple Biometric Grand Challenge [23]. The data presented in this event comprised two kinds of near infrared iris videos. The first kind of videos was captured via an LG 2200 camera, while the second kind of videos included iris and face information that were captured via a Sarnoff Iris on the Move portal [20].

A limited researching effort have been made using the MBGC data such as some introductory results that were provided at a workshop [22]. Moreover, three conference papers on the topic were the outcomes of a very recent International Conference in Biometrics. The first of these three papers was our early version of this research [12]. The other two papers were written by Lee et al. [15] and Nsaef et al. [33] respectively. These two papers offered techniques of eyes detection in the MBGC portal videos and then evaluate the quality of the obtained eye images. They made a comparison between portal iris videos and still images. At a false accept rate of 0.80%, they achieved a false reject rate of 43.90%.

A later work by Zhou et al. [32] explored the MBGC iris video data suggesting adding some specifications to the old iris system so as to choose the best frames from the video. Each frame will be first inspected for blink, interlacing and blur. After that interpolation is used to correct deinterlacing. Later, blurry frames and frames without an eye are rejected. Frames which have been chosen for segmentation in the traditional procedure are later allocated a confidence score based on the quality of the segmentation. Zhou et al. further assessed the quality by checking differences in iris texture, the quantity of occlusion as well as the quantity of dilation. They classified iris videos into five sets on the basis of quality score. They concluded that a higher quality score correlated with a lower equal error rate.

This paper focuses on the selection of the best frame from a video to be used in consequent handling. This paper also aims to properly detect the pupil borders from the iris image. That means detecting the locations of the center and radius of the pupil and later segmenting the outer of iris via (GAC) algorithm.

### 3. DATA

Government of the U.S planned for the Multiple Biometric Grand Challenge [23]. The data presented in this event comprised two kinds of near infrared iris videos. The first kind of videos was captured via an LG 2200 camera, while the second kind of videos included iris and face information that were captured via a Sarnoff Iris on the Move portal [20]. The first type of MBGC NIR Video is used in this paper.

There are 290 videos in the NIR Video dataset with 113 subjects and with a number of frames extending from 5 to 1018 a video. The clips should be in MPEG-4 format and all videos should include one of the two eyes only.

This work presents a method that aims at consistently handling iris videos in a way that frames of the best quality are the ones selected.

First, the frames of video capture and storage in the form of images format jpg then apply the root mean square (RMS) to identify the image contrast and the denied of all frames have bad contrast and then identify whether they have pictures blockage to refuse or do not have to accept and then determine blur all pictures that have accepted from the previous step by applying the measure curvature focus Helmlli [11] and then choose the best 10 images from video ever to be to create a database of the 2230 picture.

### 4. PROPOSED IRIS SEGMENTATION

In the system of iris recognition, pupil and outer boundary segment should be accurate and fast. Pupil part is clearly dissimilar from the rest of the grey scale eye image area. The eye pupil could be thought of a circular shape; hence, it is displayed as a dark rounded area inside the iris. The eye image (I) is brought down and thresholded producing a binary image (It) to purify pupil pixels. It decreases the search space for the iris inner boundary of the pupil to include only the dark pixels in the image. First, this technique dynamically (I) defines the zone of attention (ZOA) This ZOA is the area where the pupil border result algorithm will begin.

In order to implement this automation we analyze the histogram graph gray scale that is used to monitor the distribution of the pixel density of the complete picture. We know in advance that the density of the pupils in the gray scale is close to zero [3]. To assess the value of the region pupil performs an algorithm which analyzes the peaks and valleys on the chart. This technique is applied filter media to the histogram, and calculates the cliffs for the detection of summits on the histogram. Figs. 1 discern between the two histograms extracted from two different two pictures from the video eye MBGC database.

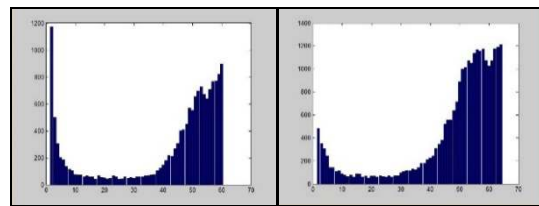


Figure 1: Histogram Extracted From Two Different Two Pictures From The Video Eye MBGC Database.

The first summit is deemed as the worth of the severity of the pupil. Equation (1) is use to determine dynamically the region of interest where the pupil is,

$$f(x,y) = \begin{cases} 0, I(x,y) < h_1 \\ 1, otherwise \end{cases} \quad (1)$$

Where  $f(x, y)$  is the resulting image,  $I(x, y)$  is the intensity value of each pixel in image and  $h_1$  is the value of the first summit.

However, serious problems arise due to several kinds of noise pixels such as eyelashes, eyebrows, specular or shadow reflections on the pupil. Holes from (It) can be eliminated using the morphological flood-filling operator. In order to get the binary image (Itf), shiny reflection within the region of the pupil and other dark patches resulting from eyelashes should be also eliminated. The following figure shows two different pictures eye after applying the threshold of closing with opining and Fill holes image morphology the conformation.

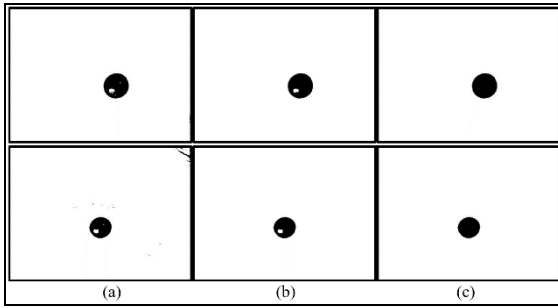


Figure 2: a) Thresholding. b) Closing & Opening. c) Fill holes image

After using that improved circular Hough transform to identify the inner border, the search space of the standard circular Hough transform will be decreased. It used to include three dimensions; the center, the coordinates and the radius. It will now only include one dimension that is the radius. Time complexity of this improved Hough transform will be significantly decreased in accordance to search space reduction.

All dark pixels in Image are skimmed for pixel (P) to obtain the true value, and the center is found by the use of the equations below:

$$\begin{aligned} xc &= x - r * \cos(\theta) \\ yc &= y - r * \sin(\theta) \end{aligned} \quad (2)$$

Where x, y are the coordinates at pixel P and r is the probable range of the values of the radius which is [25:75], and  $\theta$  range is [0:  $\pi$ ]. The pupil segmentation is shown in Figure 3 below:

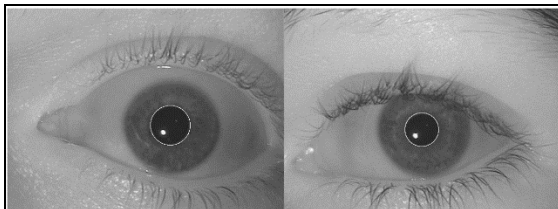


Figure 3: Pupil Segmentation

After that the Geodesic Active Contours will be applied to segment outer boundary. The approach proposed by Shah and Ross [28], is grounded on the relationship between active contours and the computation of geodesics (least length curves). The plan is to develop a randomly modified curve from the iris due to the impact of geometric features of the iris boundary. GACs work on combining the approach that minimizes the energy of the

traditional “snakes” and the geometric active contours that is based on curve evolution.

Figure below presented the enhance GAC for iris segmentation.

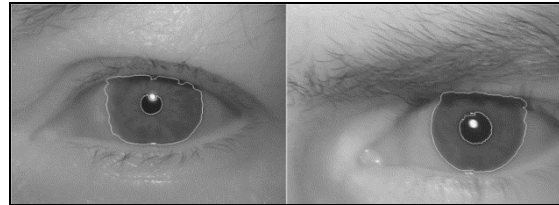


Figure 4: Segmenting MBGC VI Video Still iris Irides Using GAC.

## 5. NORMALIZATION

The concept of rubber sheet modal proposed by Daugman [7] was used at this stage. Since it was unpacked, it altered the Cartesian coordinate system and mapped all the points inside the iris boundary into their Polar counterparts. This rubber sheet modal can be described in the following equation:

$$I(X(r, \theta), y(r, \theta)) \rightarrow (r, \theta) \quad (3)$$

Where I(x, y) is known as the iris image of the region, and both (x, y) refer to the original Cartesian coordinates

## 6. FEATURES EXTRACTION AND ENCODING

The 2D normalized pattern is made into several 1D signals in this process, and theconvolve is implemented between the 1D signals and 1D Log-Gabor wavelets. Consequently, the lines of the normalized 2d patterns are regarded as the 1D signal such that each line represents a rounded ring on the region of the iris. The LogGabor Filters D. Field [10] was used at seven stages. The Log-Gabor Filters is outlined as in the equation below:

$$G(f) = \exp\left(\frac{-(\log(f/f_0))^2}{(\log(\sigma/f_0))^2}\right) \quad (4)$$

Where  $f_0$  is a representation of the center frequency and  $\sigma$  provides the bandwidth of the filter.

## 7. CLASSIFICATION AND MATCHING

The last stage in iris recognition procedure required the employment of the Hamming distance (HD) test that was conducted by means of a

comparison between the iris code calculated in real time and the iris code in a saved file. The comparison made in this study was intended to compare between calculated iris code and codes in the MBGC v1 NIR Video database. The formula of the Hamming distance is provided in the following equation, where X and Y, are the two iris code sequences and the Hamming distance is presented as given below.

$$HD = \frac{1}{N} \sum_{i=1}^N X_i \oplus Y_i \quad (5)$$

Where  $X_i$  and  $y_i$  refers to the  $i$ -th bit in the iris code sequence X and Y, and N is the total number of bits in each iris code sequence. The symbol “XOR” refers to the operator.

### 8. RESULT AND DISCUSES

Table (1) below discern the compare of the time segmented of pupil between performed algorithm of “dynamic threshold” and open source masek [19] algorithm.

Table 1: execution time of pupil segmentation

number of pictures	name of pictures	execution time depends on masek [14]	execution time depends on Our method
1	S1001R01	13.0311	0.2266
2	S1002L07	8.7598	0.2005
3	S1006L01	35.1082	0.2110
4	S1042L01	17.7921	0.1954
5	S1050L01	19.8923	0.1875
6	S1058L02	15.2073	0.1922
7	S1063R01	24.7699	0.1924
8	S1093R01	17.5187	0.1947
9	S1079R02	27.3801	0.2160
10	S1095R05	6.9382	0.2620
Average time		18.63977	0.20783

From the above table (1) that monitor the processing time segmented the pupil by the our method that depends on the “dynamic threshold” that has taken less execution time than masek [19] algorithm, where the rate time of the pupil segmented depends on our method “dynamic threshold” is 0.20783 seconds, while the rate time a pupil segmented using masek [19] method is 18.63977 second. Therefore, the proposed method which is depending on a “dynamic threshold” is faster.

Below in appendix see Figure 5 present several the segmented of the pupil for iris picture taken from the MBGC V1 NIR Video database depend on our

method “dynamic threshold” and masek [19] respectively

We can see in figure 5 our method “dynamic threshold” have not erroneous segment and on other side show the maske [19] method have abundant erroneous segment. Based on table 1 and figure 5 we can deduce that our method “dynamic threshold” is more speed and exact than masek [19] method.

In this study, the dataset in the “MBGC v1 NIR Video database” was tested by choice of four (4) pictures from the left and four (4) pictures of the right of every individual. However, the use of the residual pictures in the “ MBGC V1 NIR Video database” for the purpose of training, which was chosen six (6) pictures form the left and six (6) other pictures of the right of every individual “training data”.

The result received by our execution on the grounds geodetic active contour [28] (GAC) with a precision 98.4305% recognition rate. As indicated in the picture below

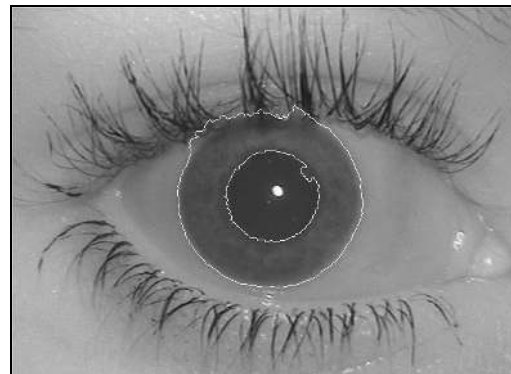


Figure 6: Image getting on the grounds our execution “Geodesic Active Contour [28] (GAC)”

The result received by our execution on the masek [19] with a precision 98.4305% recognition rate. As indicated in the picture below

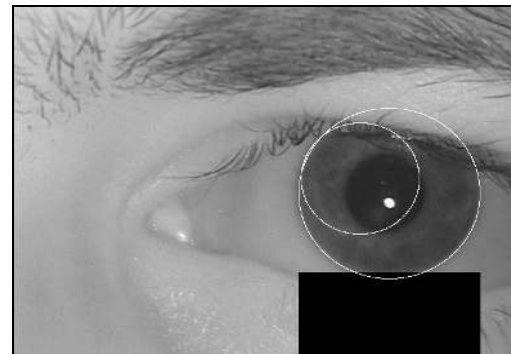


Figure 7: Image getting on the grounds our execution “masek [19]”



In appendix below see “Mean” (M), “standard deviation” (STD) and “degree of freedom” (DOF) for GAC in the tables 2, 3, 4 respectively and for open source masek [19] method in the tables 5, 6, 7 respectively

The grounds on the tables 2-7 us can deduce that when increase the Mean the Standard division is decrease and increase the degrees of freedom. The number of degrees of freedom indicates that the differences between two irises are good.

## 9. CONCLUSION:

An optimal frame selection technique was proposed in this study to enhance the efficiency of iris recognition systems that are based on videos. The current study revealed that the proposed method on the grounds of “dynamic threshold” for pupil segmentation is carried out to increase the speed and accurate recognition rate. Also Geodesic Active Contour Algorithm is proposed for outer boundary segment, which is similar to some well-known works such as the masek method. However, the present study was limited to certain aspects. Some other beneficial aspects were also indicated as potential ideas for future research.

## REFERENCES:

- [1] W. W. Boles, and B. Boashash, "A human identification technique using images of the iris and wavelet transform", *IEEE transactions on signal processing*, vol. 46, no. 4, 1998, pp. 1185-1188.
- [2] K. W. Bowyer, K. Hollingsworth, and P. J. Flynn, "Image understanding for iris biometrics: A survey", *Computer vision and image understanding*, vol. 110, no. 2, 2008, pp. 281-307.
- [3] Y. Chen, J. Wang, C. Han *et al.*, "A robust segmentation approach to iris recognition based on video", *Applied Imagery Pattern Recognition Workshop, 2008. AIPR'08. 37th IEEE*, 2008, pp. 1-8.
- [4] J. Daugman, "High confidence recognition of persons by iris patterns", *Security Technology, 2001 IEEE 35th International Carnahan Conference on*, 2001, pp. 254-263.
- [5] J. Daugman, "How iris recognition works", *Circuits and Systems for Video Technology, IEEE Transactions on*, vol. 14, no. 1, 2004, pp. 21-30.
- [6] J. Daugman, "New methods in iris recognition", *IEEE Transactions on Systems, Man, and Cybernetics, Part B*, vol. 37, no. 5, 2007, pp. 1167-1175.
- [7] J. G. Daugman, "High confidence visual recognition of persons by a test of statistical independence", *Pattern Analysis and Machine Intelligence, IEEE Transactions on*, vol. 15, no. 11, 1993, pp. 1148-1161.
- [8] Y. Du, "Using 2D log-Gabor spatial filters for iris recognition", *Defense and Security Symposium*, 2006, pp. 62020F-62020F-62028.
- [9] Y. Du, R. W. Ives, D. M. Etter *et al.*, "Use of one-dimensional iris signatures to rank iris pattern similarities", *Optical Engineering*, vol. 45, no. 3, 2006, pp. 037201-037201-037210.
- [10] D. J. Field, "Relations between the statistics of natural images and the response properties of cortical cells", *JOSA A*, vol. 4, no. 12, 1987, pp. 2379-2394.
- [11] F. S. Helml, and S. Scherer, "Adaptive shape from focus with an error estimation in light microscopy", *Image and Signal Processing and Analysis, 2001. ISPA 2001. Proceedings of the 2nd International Symposium on*, 2001, pp. 188-193.
- [12] K. P. Hollingsworth, K. W. Bowyer, and P. J. Flynn, "Image averaging for improved iris recognition", *Advances in Biometrics*, vol., no., 2009, pp. 1112-1121.
- [13] N. D. Kalka, J. Zuo, N. A. Schmid *et al.*, "Estimating and fusing quality factors for iris biometric images", *Systems, Man and Cybernetics, Part A: Systems and Humans, IEEE Transactions on*, vol. 40, no. 3, 2010, pp. 509-524.
- [14] E. Krichen, L. Allano, S. Garcia-Salicetti *et al.*, "Specific texture analysis for iris recognition", *Audio-and Video-Based Biometric Person Authentication*, 2005, pp. 23-30.
- [15] Y. Lee, P. J. Phillips, and R. J. Micheals, "An automated video-based system for iris recognition", *Advances in Biometrics*, vol., no., 2009, pp. 1160-1169.
- [16] L. Ma, T. Tan, Y. Wang *et al.*, "Personal identification based on iris texture analysis", *Pattern Analysis and Machine Intelligence, IEEE Transactions on*, vol. 25, no. 12, 2003, pp. 1519-1533.
- [17] L. Ma, T. Tan, Y. Wang *et al.*, "Efficient iris recognition by characterizing key local variations", *Image Processing, IEEE Transactions on*, vol. 13, no. 6, 2004, pp. 739-750.
- [18] N. K. Mahadeo, A. P. Papiński, and S. Ray, "Model-based pupil and iris localization", *Neural Networks (IJCNN), The 2012 International Joint Conference on*, 2012, pp. 1-7.



- [19] L. Masek, "Recognition of human iris patterns for biometric identification", *The University of Western Australia*, vol. 2, no., 2003.
- [20] J. R. Matey, O. Naroditsky, K. Hanna *et al.*, "Iris on the move: Acquisition of images for iris recognition in less constrained environments", *Proceedings of the IEEE*, vol. 94, no. 11, 2006, pp. 1936-1947.
- [21] A. K. Nsaef, A. Jaafar, and K. N. Jassim, "Enhancement segmentation technique for iris recognition system based on Daugman's Integro-differential operator", *Instrumentation & Measurement, Sensor Network and Automation (IMSNA), 2012 International Symposium on*, 2012, pp. 71-75.
- [22] P. J. Phillips, "MBGC presentations and publications", vol., no. Issue, 2008.
- [23] P. J. Phillips, P. J. Flynn, J. R. Beveridge *et al.*, "Overview of the multiple biometrics grand challenge", *Advances in Biometrics*, vol., no., 2009, pp. 705-714.
- [24] H. Proenca, and L. A. Alexandre, "Toward noncooperative iris recognition: a classification approach using multiple signatures", *Pattern Analysis and Machine Intelligence, IEEE Transactions on*, vol. 29, no. 4, 2007, pp. 607-612.
- [25] K. Roy, P. Bhattacharya, and C. Y. Suen, "Towards nonideal iris recognition based on level set method, genetic algorithms and adaptive asymmetrical SVMs", *Engineering Applications of Artificial Intelligence*, vol. 24, no. 3, 2011, pp. 458-475.
- [26] N. A. Schmid, M. V. Ketkar, H. Singh *et al.*, "Performance analysis of iris-based identification system at the matching score level", *Information Forensics and Security, IEEE Transactions on*, vol. 1, no. 2, 2006, pp. 154-168.
- [27] S. A. Schuckers, N. A. Schmid, A. Abhyankar *et al.*, "On techniques for angle compensation in nonideal iris recognition", *Systems, Man, and Cybernetics, Part B: Cybernetics, IEEE Transactions on*, vol. 37, no. 5, 2007, pp. 1176-1190.
- [28] S. Shah, and A. Ross, "Iris segmentation using geodesic active contours", *Information Forensics and Security, IEEE Transactions on*, vol. 4, no. 4, 2009, pp. 824-836.
- [29] M. Vatsa, R. Singh, and A. Noore, "Improving iris recognition performance using segmentation, quality enhancement, match score fusion, and indexing", *Systems, Man, and Cybernetics, Part B: Cybernetics, IEEE Transactions on*, vol. 38, no. 4, 2008, pp. 1021-1035.
- [30] R. P. Wildes, "Iris recognition: an emerging biometric technology", *Proceedings of the IEEE*, vol. 85, no. 9, 1997, pp. 1348-1363.
- [31] S. K. Zhou, and R. Chellappa, "Beyond one still image: Face recognition from multiple still images or a video sequence", *Face Processing: Advanced Modeling and Methods*, vol., no., 2005, pp. 547-567.
- [32] Z. Zhou, Y. Du, and C. Belcher, "Transforming traditional iris recognition systems to work in nonideal situations", *Industrial Electronics, IEEE Transactions on*, vol. 56, no. 8, 2009, pp. 3203-3213.
- [33] A. K. Nsaef, A. Jaafar, L. Sliman *et al.*, "Model of Bayesian tangent eye shape for eye capture", *Intelligent Systems Design and Applications (ISDA), 2014 14th International Conference on*, 2014, pp. 82-88.
- [34] A. K. Nseaf, A. Jaafar, H. Rashid *et al.*, "Design method of video based iris recognition system (V-IRS)," *Advances in Visual Informatics, 2013*, pp. 526-538.

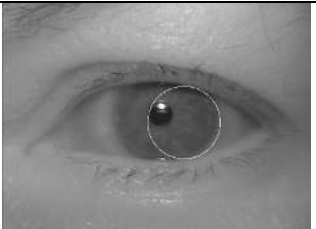
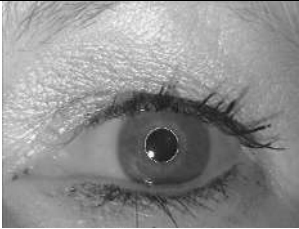
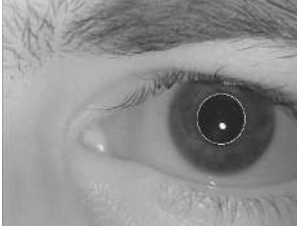
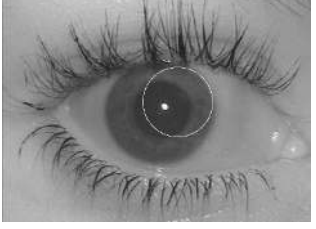
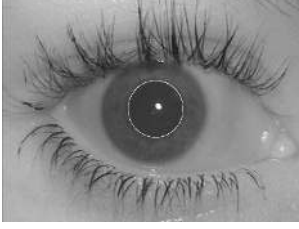
numeral Of pictures	Original picture	Pupil segment depends on (mask 2003)	Pupil segment depends on Our method
S1002L07			
S1006L01			
S1058L02			
S1079R02			
S1095R05			

Figure 5: Pupil Segment



Table.2 Mean Of The “MBGC VI NIR Video Database” With Different Template Ratio Of Distance Using GAC

Template	40	80	120	160	200	240	280	320	512
4	0.440796	0.468360	0.480632	0.484550	0.486573	0.487930	0.488927	0.489757	0.492203
8	0.447252	0.473073	0.484323	0.487834	0.489684	0.490863	0.491696	0.492358	0.494280
12	0.449217	0.474271	0.485403	0.488864	0.490684	0.491857	0.492669	0.493313	0.495194
16	0.449857	0.474793	0.485836	0.489302	0.491129	0.492288	0.493127	0.493774	0.495653
20	0.450553	0.475188	0.486105	0.489557	0.491365	0.492529	0.493361	0.494033	0.495910
24	0.450696	0.475348	0.486246	0.489690	0.491481	0.492670	0.493498	0.494170	0.496069
28	0.450962	0.475462	0.486341	0.489767	0.491570	0.492750	0.493593	0.494260	0.496164
32	0.451069	0.475534	0.486403	0.489833	0.491616	0.492796	0.493644	0.494310	0.496223
64	0.451217	0.475740	0.486544	0.489942	0.491738	0.492914	0.493759	0.494424	0.496347

Table.3 Stander Deviation Of The “MBGC VI NIR Video Database” With Different Template Ratio Of Distance Using GAC

Template	40	80	120	160	200	240	280	320	512
4	0.081695	0.050205	0.038750	0.033938	0.030738	0.028359	0.026523	0.025031	0.020093
8	0.073666	0.042827	0.031510	0.026774	0.023727	0.021524	0.019886	0.018581	0.014591
12	0.070945	0.040692	0.029466	0.024777	0.021742	0.019512	0.017824	0.016502	0.012479
16	0.069846	0.039668	0.028532	0.023933	0.020893	0.018633	0.016908	0.015567	0.011477
20	0.068906	0.039108	0.028073	0.023439	0.020414	0.018143	0.016419	0.015065	0.010889
24	0.068445	0.038834	0.027810	0.023170	0.020140	0.017874	0.016147	0.014791	0.010583
28	0.068182	0.038612	0.027620	0.023011	0.019985	0.017726	0.015999	0.014624	0.010405
32	0.067993	0.038486	0.027506	0.022905	0.019884	0.017626	0.015898	0.014533	0.010289
64	0.067444	0.038120	0.027213	0.022635	0.019632	0.017383	0.015657	0.014294	0.010042

Table.4 Degree Of Freedom Of The “MBGC VI NIR Video Database” With Different Template Ratio Of Distance Using GAC

Template	40	80	120	160	200	240	280	320	512
4	37	99	166	217	264	311	355	399	619
8	46	136	252	349	444	539	632	724	1174
12	49	151	288	407	529	656	787	918	1605
16	51	158	307	436	573	720	874	1031	1898
20	52	163	317	455	600	759	927	1101	2108
24	53	165	323	465	616	782	959	1143	2232
28	53	167	327	472	626	795	976	1169	2309
32	54	168	330	476	632	805	989	1184	2361
64	54	172	337	488	648	827	1020	1223	2479

Table.5 Mean Of The “MBGC VI NIR Video Database” With Different Template Ratio Of Distance Using Open Source Masek [19]

Template	40	80	120	160	200	240	280	320	512
4	0.431682	0.473284	0.481098	0.484109	0.486167	0.487567	0.488624	0.489453	0.491907
8	0.436394	0.477211	0.484860	0.487701	0.489446	0.490638	0.491490	0.492158	0.494160
12	0.437988	0.477402	0.485633	0.488599	0.490422	0.491658	0.492503	0.493169	0.495088
16	0.438011	0.477279	0.485864	0.490837	0.488996	0.492087	0.492961	0.493636	0.495545
20	0.438268	0.477252	0.485973	0.489180	0.491072	0.492303	0.493188	0.493883	0.495816
24	0.438385	0.477238	0.485991	0.489279	0.491187	0.492450	0.493339	0.494034	0.495998
28	0.438489	0.477184	0.486053	0.489353	0.491271	0.492532	0.493431	0.494120	0.496102
32	0.438482	0.477117	0.486050	0.489395	0.491324	0.492597	0.493487	0.494179	0.496156
64	0.438731	0.476972	0.486028	0.489485	0.491445	0.492726	0.493628	0.494327	0.496316



Table.6 Stander Deviation Of The “MBGC V1 NIR Video Database” With Different Template Ratio Of Distance Using Open Source Masek [19]

Template	40	80	120	160	200	240	280	320	512
4	0.088076	0.053674	0.040829	0.035198	0.031681	0.029166	0.027291	0.025755	0.020594
8	0.079850	0.046058	0.033520	0.027807	0.024318	0.021944	0.020275	0.018967	0.014874
12	0.076719	0.043901	0.031411	0.025722	0.022197	0.019763	0.018033	0.016704	0.012625
16	0.075223	0.042897	0.030518	0.021285	0.024814	0.018839	0.017063	0.015703	0.011558
20	0.074454	0.042312	0.030007	0.024299	0.020772	0.018297	0.016522	0.015126	0.010929
24	0.074042	0.042056	0.029724	0.024017	0.020484	0.018012	0.016216	0.014828	0.010584
28	0.073669	0.041858	0.029501	0.023833	0.020302	0.017828	0.016029	0.014638	0.010378
32	0.073366	0.041716	0.029384	0.023710	0.020191	0.017706	0.015911	0.014526	0.010259
64	0.072603	0.041267	0.029007	0.023364	0.019855	0.017390	0.015596	0.014215	0.009954

Table.7 Degree Of Freedom Of The “MBGC V1 NIR Video Database” With Different Template Ratio Of Distance Using Open Source Masek [19]

Template	40	80	120	160	200	240	280	320	512
4	32	87	150	202	249	294	335	377	589
8	39	118	222	323	423	519	608	695	1130
12	42	129	253	378	507	640	769	896	1568
16	44	136	268	552	406	704	859	1014	1871
20	44	139	277	423	579	747	916	1092	2093
24	45	141	283	433	596	770	951	1137	2232
28	45	142	287	440	606	786	973	1167	2321
32	46	143	289	445	613	797	987	1185	2375
64	47	146	297	458	634	826	1028	1237	2523